ISSN 1070-4272, Russian Journal of Applied Chemistry, 2017, Vol. 90, No. 8, pp. 1278−1284. © Pleiades Publishing, Ltd., 2017.
Original Russian Text © D.A. Krainova, S.T. Zharkinova, N.S. Saetova, A.A. Raskovalov, A.V. Kuz'min, V.A. Eremin, E.A. Sherstobitova, S.V. Pershina, M.V. Dyadenko, Xiaoa Zhang, Shengling Jiang, 2017, published in Zhurnal Prikladnoi Khimii, 2017, Vol. 90, No. 8, pp. 1047−1053.

VARIOUS TECHNOLOGICAL PROCESSES

Influence of Cerium Oxide on Properties of Glass–Ceramic Sealants for Solid Oxide Fuel Cells

D. A. Krainova[a,b], S. T. Zharkinova[a], N. S. Saetova[a], A. A. Raskovalov[a], A. V. Kuz'min[a,b]*, V. A. Eremin[a,b], E. A. Sherstobitova[a,c], S. V. Pershina[a], M. V. Dyadenko[d], Xiaoa Zhang[e], and Shengling Jiang[e]

[a] *Institute of High-Temperature Electrochemistry, Ural Branch, Russian Academy of Sciences, Yekaterinburg, Russia*
[b] *Yeltsin Ural Federal University, Yekaterinburg, Russia*
[c] *Institute of Metal Physics, Ural Branch, Russian Academy of Sciences, Yekaterinburg, Russia*
[d] *Belarussian State University of Technology, Minsk, Belarus*
[e] *Key Laboratory of Carbon Fiber and Functional Polymers of Ministry of Education, College of Materials Science and Engineering, Beijing University of Chemical Technology, Beijing, China*
**e-mail: a.v.kuzmin@yandex.ru*

Received September 28, 2017

Abstract—The influence of the cerium oxide concentration on the properties of glasses and glass ceramics of the SiO_2–Al_2O_3–CaO–Na_2O–MgO–K_2O–B_2O_3–CeO_2 system as potential adhesive and sealing materials for solid oxide fuel cells was studied. According to the data of differential scanning calorimetry, variation of the CeO_2 concentration does not appreciably influence the glass transition and crystallization temperatures of glasses. As the cerium oxide concentration is increased, the linear thermal expansion coefficient increases for the glasses but decreases for the partially crystalline samples. The gluing temperature of the glass sealants prepared allows their use for joining YSZ solid electrolytes with interconnectors of Crofer22APU type in solid oxide fuel cells..

DOI: 10.1134/S1070427217080146

The development of a sealant preventing mixing of gases and fuel in the course of solid oxide fuel cell (SOFC) operation is one of the key problems to be solved in the development of stably operating SOFCs [1]. Numerous requirements are imposed upon sealants for SOFCs. These include chemical stability in both oxidizing and reducing atmospheres, high electrical resistance to avoid shorting between cell components, appropriate linear thermal expansion coefficient (LTEC), capability to operate at high temperatures (800–1000°C) for a long time, etc. [2, 3]. Glasses and glass ceramics meeting to a sufficient extent all the requirements imposed upon SOFC sealants show promise in this respect [4]. The advantage of glassy sealants is that glasses at high temperatures of SOFC operation are in the viscous-flow state, which reduces the mechanical stress between SOFC components [5, 6]. However, the possibility of partial or complete crystallization of glass in the course of SOFC operation is its drawback. It leads to a decrease in the glass viscosity and can cause cracking of the sealant, which, in turn, will make the whole structure untight [7–10]. Furthermore, glass can chemically interact with the interconnector material [11]. However, despite these drawbacks, high-temperature silicate glasses proved themselves as sealing materials withstanding the SOFC operation conditions for 1000 h without significant degradation of properties [12–14].

There are numerous studies dealt with alkaline aluminosilicate glasses as materials for SOFC sealants. Chou et al. tested Al–Ba–Ca–K–Na–Si and Sr–Ca–Y–B–Si glasses as potential SOFC sealants [15–17]. In particular, Al–Ba–Ca–K–Na–Si glasses in contact with YSZ and with AI-SI441 ferrite stainless steel were studied [15]; it was found that the glass remained chemically stable and did not enter into any reactions in the course of keeping at 750°C for 1000 h or cycling in the temperature interval 50–750°C with a heating rate

of 5 deg min^{-1}. The behavior of Al–Ba–Ca–K–Na–Si in contact with YSZ and SS441 aluminized stainless steel under the conditions of keeping at 750 and 800°C for 1000 h in a 5% H_2/N_2 stream was studied in [16]. No signs of the reaction of the glass with YSZ ceramic and with SS441 steel were detected after the experiment completion. Sr–Ca–Y–B–Si glasses were also studied in contact with YSZ ceramic and with AI-SI441 ferrite stainless steel. In the stack assembled from three unit cells, the glass degraded at the operation temperature of 800°C to form $SrCrO_4$ because of the presence of chromium impurity in the steel [17].

Qi et al. [18] studied as sealants glasses of the compositions $45SiO_2{-}15Al_2O_3{-}25BaO{-}15MgO$ and $60SiO_2{-}10Al_2O_3{-}10ZrO_2{-}5CaO{-}15Na_2O$. As they found, the use of the $SiO_2{-}Al_2O_3{-}ZrO_2{-}CaO{-}Na_2O$ glass as a sealant is preferable, because it is chemically resistant to Crofer22APU alloy. The stability of the $54.39SiO_2{-}11.26Al_2O_3{-}9.02CaO{-}13.78Na_2O{-}8.37MgO{-}1.67K_2O{-}0.9B_2O_3{-}0.61Y_2O_3$ glassy sealant in contact with $Mn_{1.5}Co_{1.5}O_4$-coated Crofer22APU and with YSZ ceramic was studied in [2]. This glass was found to be promising for use in SOFCs, because it has suitable linear thermal expansion coefficient (8.5×10^{-6} and 10.9×10^{-6} K^{-1} for the initial glass and for the glass ceramic, respectively) and does not react with the interconnector material after 500-h cycling in the interval 25–850°C. It should be noted, however, that there are rare pores in the bulk of this glass, which can lead to degradation of the material in the course of longer operation at high temperatures.

This study deals with the influence exerted by the cerium oxide concentration on the properties of $SiO_2{-}Al_2O_3{-}CaO{-}Na_2O{-}MgO{-}K_2O{-}B_2O_3{-}CeO_2$ glasses, which are of interest as glassy sealants for SOFCs.

EXPERIMENTAL

As components of the batch for preparing the glasses, we used $CaCO_3$ (chemically pure grade), Na_2CO_3 (chemically pure grade), SiO_2 (hydrous), K_2CO_3 (ultrapure grade), B_2O_3 (ultrapure grade), MgO (ultrapure grade), Al_2O_3 (ultrapure grade), and CeO_2 (chemically pure grade), preliminarily calcined to constant weight. The component ratios corresponded to the calculated compositions given in Table 1. We studied four glass compositions (denoted as $0.61Y_2O_3$, $0.61CeO_2$, $1.0CeO_2$, and $2.0CeO_2$). The component ratio in the cerium-free formulation was taken from [2]; the other formulations were obtained by replacing first yttrium oxide and then also partially aluminum oxide by cerium oxide. The batch was calcined at 600°C for 30 min, after which it was cooled to room temperature and pressed in pellets 10 mm in diameter. Corundum crucibles filled by 3/4 were placed in a LinnHighTherm HT 1800 furnace with $MoSi_2$ heaters.

To obtain the maximum homogeneous glass, we used stepwise heating schedule. In the first step, the furnace was heated to 1050°C over a period of 3 h and kept at this temperature for 30 min. Then, the temperature was raised to 1400°C over a period of 1 h, and the melt was kept at this temperature for 3 h. In the third and fourth steps, the furnace was heated to 1450 and 1480°C, respectively, over a period of 15 min and kept at these temperatures for 15 min. Glass samples were prepared by casting the melt into a glassy carbon mold. To relieve thermal stresses, the glass was annealed at 575°C for 20 min, with the subsequent slow cooling to room temperature.

The chemical composition of the glasses was determined by X-ray fluorescence spectroscopy (XFS). Measurements were performed with a Shimadzu XRF-1800 consecutive wave-dispersive X-ray fluorescence spectrometer.

To confirm the amorphous structure of the samples and study the phase composition of the crystallized glasses, we used X-ray diffraction analysis. Measurements were performed in the interval $2\theta = 10°–70°$ with a Rigaku DMX2200 diffractometer with a vertical goniometer and a graphite monochromator using CuK_α radiation.

To find LTEC of the samples, we performed measurements with a Tesatronic TT-80 dilatometer equipped with a TESAGT 21HP probe (measurement interval ±200 μm, sensitivity 0.01 μm) in the temperature interval 50–600°C. LTEC is defined as the derivative of the linear expansion with respect to temperature. Therefore, it is convenient to calculate LTEC by presenting the temperature dependence of the relative expansion Y in the form of a certain function and then differentiating it analytically. In our case, the experimental data in the interval 298–673 K are well described by the following function:

$$\frac{\Delta l}{l_0} = Y(T) = a + bT + cT^2 + \frac{d}{T}, \qquad (1)$$

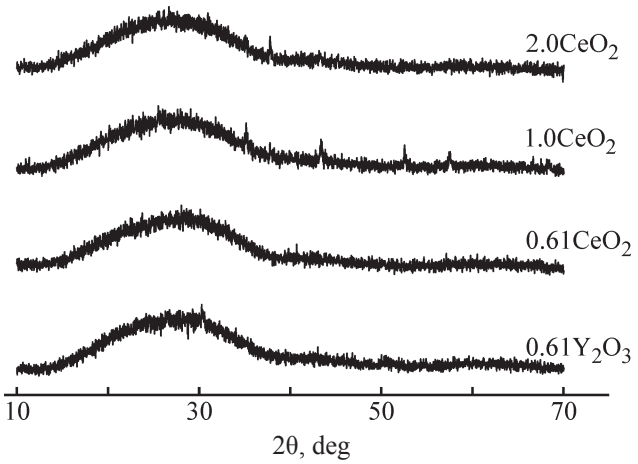

Fig. 1. X-ray diffraction patterns of SiO_2–Al_2O_3–CaO–Na_2O–MgO–K_2O–B_2O_3–Y_2O_3–CeO_2 glasses after the synthesis. (2θ) Bragg angle; the same for Figs. 2 and 5.

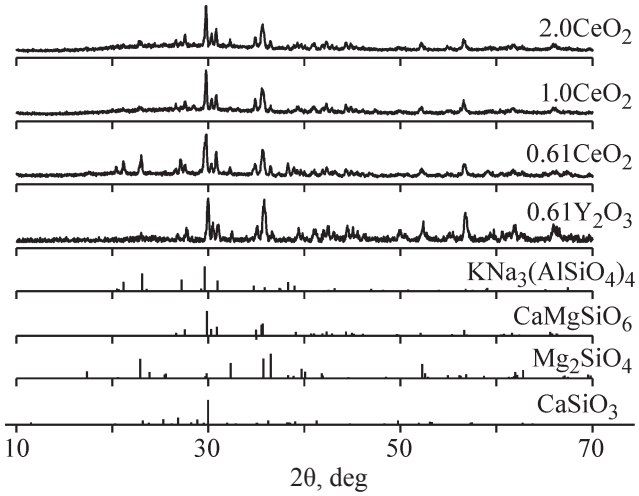

Fig. 2. X-ray diffraction patterns of samples pressed from the glass powder after annealing.

where T is the absolute temperature, and a, b, c, and d are empirical coefficients.

Hence, LTEC (α), which is the derivative of function (1), will be described by the function

$$\alpha(T) = \frac{\mathrm{d}Y}{\mathrm{d}T} = b + 2cT - \frac{d}{T^2}. \quad (2)$$

The mean value of α in a certain temperature interval can be found from expression (2). The problem is solved by integration over this temperature interval and division by the width of this interval:

$$\bar{\alpha} = \frac{1}{T_2 - T_1}\int_{T_1}^{T_2} \alpha(T)\mathrm{d}T, \quad (3)$$

where T_1 and T_2 are the boundaries of the temperature interval.

For the chosen temperature interval, we obtain

$$\bar{\alpha} = \frac{1}{673-298}\left[b(673-298) + c(673^2 - 298^2) + d\left(\frac{1}{673} - \frac{1}{298}\right)\right]. \quad (4)$$

The characteristic temperatures of crystallization and glass transition were determined by differential scanning calorimetry (DSC) with an STA 449 F1 Jupiter thermal analyzer (Netzsch). Measurements were performed in platinum crucibles in an argon atmosphere (flow rate 20 mL min^{-1}). The heating rate was 10 deg min^{-1}; measurements were performed in the temperature interval 50–950°C. Analysis of the DSC spectra and peak separation were performed using the Netzsch program package.

To determine the gluing temperature, the preliminarily prepared glass powder mixed with ethanol was applied onto a ceramic support made of yttria-stabilized zirconia (YSZ). The gluing temperature was determined in a tubular furnace under the conditions of heating to a preset temperature, keeping at this temperature for 10 min, and cooling. The temperature at which a smooth homogeneous glass drop well wetting the surface was formed was considered as the gluing temperature.

The microstructure of the materials was examined with a MIRA 3 LMU scanning electron microscope (Tescan, Czechia) equipped with an INCA Energy 350 microanalysis system with an Oxford Instruments X–MAX 80 energy-dispersive spectrometer.

RESULTS AND DISCUSSION

The compositions of the glasses studied in this work, according to the preset stoichiometry and results of X-ray fluorescence spectrometric analysis, are given in Table 1. Slight difference between the analytical data and preset composition may be due to weak scattering of X-ray radiation on light elements (B_2O_3). We have found that additions of cerium oxide influence the

Table 1. Calculated and experimentally determined (by XFS) compositions of SiO_2–Al_2O_3–CaO–Na_2O–MgO–K_2O–B_2O_3–Y_2O_3–CeO_2 glasses

Glass	Content of indicated oxide, wt %								
	SiO_2	Al_2O_3	CaO	Na_2O	MgO	K_2O	B_2O_3	Y_2O_3	CeO_2
$0.61Y_2O_3$:									
calculated composition [2]	54.39	11.26	5.02	13.78	12.37	1.67	0.9	0.61	–
XFS	55.22	11.21	5.17	14.67	10.57	1.58	0.73	0.57	–
$0.61CeO_2$:									
calculated composition	54.39	11.26	5.02	13.78	12.37	1.67	0.9	–	0.61
XFS	51.25	12.87	5.39	14.05	12.94	1.49	0.92	–	0.33
$1.0CeO_2$:									
calculated composition	54.39	10.87	5.02	13.78	12.37	1.67	0.9	–	1
XFS	52.49	12.45	5.32	14.05	12.86	1.51	–	–	0.61
$2.0CeO_2$:									
calculated composition	54.39	9.87	5.02	13.78	12.37	1.67	0.9	–	2
XFS	53.12	12.59	5.44	13.23	11.88	1.48	–	–	1.2

Table 2. Linear thermal expansion coefficients[a] calculated for the temperature interval 298–673 K

Sample	A_{theor}	A_{glass}	A_{press}
	K^{-1}		
YSZ10 solid electrolyte	9.03×10^{-6}		
Crofer22APU interconnector	10.57×10^{-6}		
$0.61Y_2O_3$	9.40×10^{-6}	9.90×10^{-6}	11.00×10^{-6}
$0.61CeO_2$	9.40×10^{-6}	9.03×10^{-6}	11.50×10^{-6}
$1.0CeO_2$	9.43×10^{-6}	9.73×10^{-6}	10.59×10^{-6}
$2.0CeO_2$	9.50×10^{-6}	9.86×10^{-6}	10.66×10^{-6}

[a] α_{theor}, LTEC of the glass, calculated using Appen method; α_{glass} and α_{press}, LTEC of the glass and glass ceramic, respectively, determined by processing dilatometric curves.

external appearance and viscosity of the glasses. For example, the sample without CeO_2 is colorless, whereas the glass with the maximal content of cerium oxide (2 wt %) is yellow. The viscosity of the melt increases with increasing CeO_2 concentration.

The amorphous structure of the samples was confirmed by X-ray diffraction analysis. Figure 1 shows the X-ray diffraction patterns of the samples. They allow a conclusion that all the samples are glassy. It should be noted, however, that in the X-ray diffraction pattern of sample $1.0CeO_2$ there are small peaks corresponding to crystalline Al_2O_3, suggesting incomplete dissolution of aluminum oxide in the glass melt.

To perform dilatometric measurements, we prepared two types of specimens: rectangular parallelepipeds cut from the bulk glass and bars pressed from the glass powder. The bars prepared by pressing were placed in a furnace, heated to 950°C, kept at this temperature for 10 min, and then slowly cooled in the furnace to room temperature. The X-ray diffraction patterns of the pressed glasses after cooling (Fig. 2) contain peaks of crystalline inclusions corresponding to the following compounds: diopside ($CaMgSi_2O_6$), wollastonite ($CaSiO_3$), nepheline [$KNa_3(AlSiO_4)_4$], and forsterite (Mg_2SiO_4). The specimens cut from the bulk glass were not subjected to additional treatment and had amorphous structure.

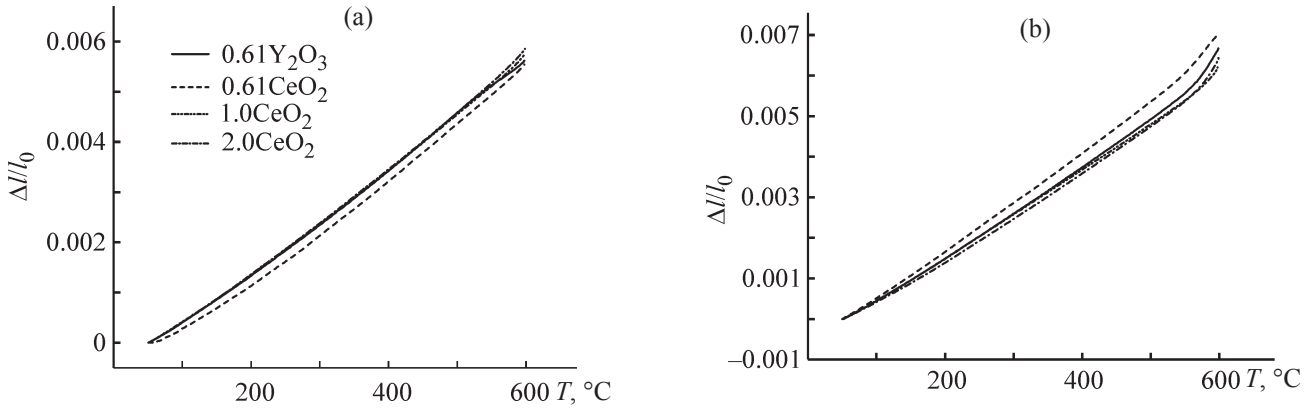

Fig. 3. Dilatometric curves obtained for (a) monolithic amorphous and (b) pressed crystalline specimens. ($\Delta l/l_0$) Relative elongation and (T) temperature.

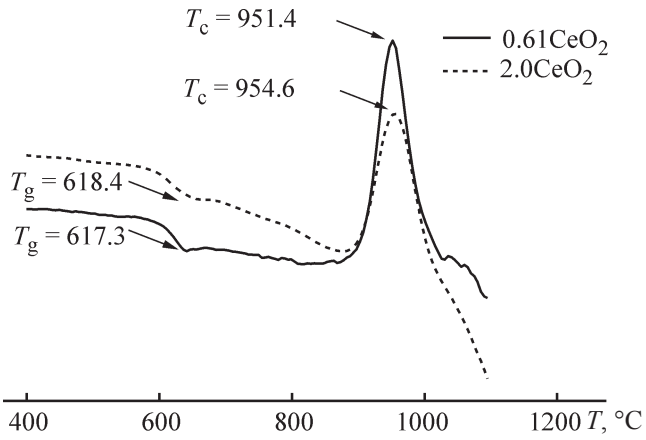

Fig. 4. DSC curves of SiO_2–Al_2O_3–CaO–Na_2O–MgO–K_2O–B_2O_3–Y_2O_3–CeO_2 glasses. (T) Temperature.

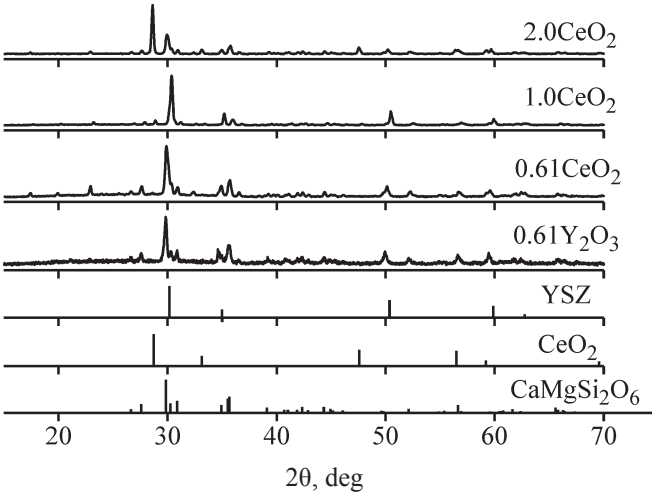

Fig. 5. X-ray diffraction patterns of samples after gluing the glass with a YSZ support.

Figure 3 shows the dilatometric curves for (a) amorphous and (b) crystalline specimens.

The values obtained by analysis of the dilatometric curves are presented in Table 2 in comparison with those for the materials used for SOFC fabrication: YSZ10 ceramic (zirconia stabilized with 10% yttria) and Crofer22APU alloy.

The dilatometric measurements show that the LTEC values for the glassy sealants studied are within the acceptable interval (α_{YSZ10}–$\alpha_{Crofer22APU}$). As the content of cerium oxide in the glass is increased, LTEC of the amorphous samples increases, whereas that of the crystalline samples decreases. Such behavior of the thermal expansion coefficient is probably associated with a change in the crystallization mechanism upon introduction of cerium oxide into the glass composition. For example, as shown in [19], introduction of even 1 mol % cerium oxide into the glass composition leads to a change in the crystallization mechanism from two- to three-dimensional. Nevertheless, our results show that replacement of yttrium and aluminum oxides by CeO_2 considerably decreases the difference between the LTEC values of the glass and SOFC materials.

Figure 4 shows the DSC data for the glasses. According to the data obtained, variation of the cerium oxide content from 0.61 to 2.0 wt % influences the glass transition, T_g, and crystallization, T_c, temperatures of the glass insignificantly.

The gluing temperatures determined from the experimental data were as follows: 1090°C for $0.61Y_2O_3$ and $0.61CeO_2$; 1100 and 1110°C for $1.0CeO_2$ and $2.0CeO_2$, respectively. On the whole, the gluing

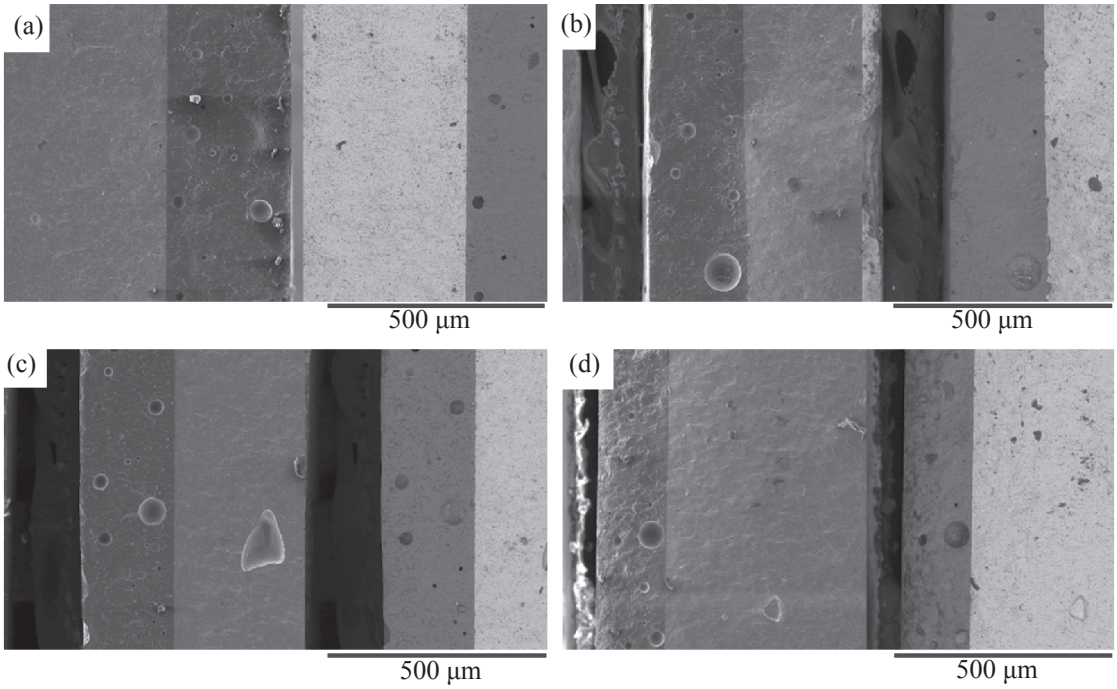

Fig. 6. Electron micrographs of chips: (a) YSZ/0.61Y_2O_3 glass, (b) YSZ/0.61CeO_2 glass, (c) YSZ/1.0CeO_2 glass, and (d) YSZ/2.0CeO_2 glass. In each part, the left and right images are taken in SET and BSE modes, respectively. Magnification 300×.

temperatures of the glassy sealants do not exceed the maximum admissible temperature for refractory alloys such as Crofer22APU and its analogs, used as SOFC interconnectors. The X-ray diffraction patterns of the samples after gluing with the ceramic support (Fig. 5) contain reflections corresponding to crystalline phases of cerium oxide, YSZ ceramic, and diopside ($CaMgSi_2O_6$).

The electron micrographs of YSZ/glass sealing couples, taken in the SEI (secondary electron) and BSE (backscattered electron) modes, are shown in Fig. 6. As can be seen, the glasses exhibit good adhesion to the material. Rare pores are seen in the bulk of the glass phase, but the porosity is not through and does not significantly affect the characteristics of the electrochemical cell.

CONCLUSIONS

(1) Properties of SiO_2–Al_2O_3–CaO–Na_2O–MgO–K_2O–B_2O_3–CeO_2 glasses were studied. An increase in the CeO_2 concentration influences the glass transition and crystallization temperatures of the glasses insignificantly. As the cerium oxide concentration is increased, the linear thermal expansion coefficient increases for amorphous and decreases for glass–ceramic samples; i.e., the difference between the linear thermal expansion coefficients of the amorphous and glass–ceramic materials decreases.

(2) The results of determining the gluing temperature of the glasses and the analysis of the electron micrographs of glass/YSZ ceramic sealing couples show that the glasses studied can be used as glassy sealants for solid oxide fuel cells, as they ensure tight gluing of the components at temperatures lower than the maximum permissible temperature for interconnector materials such as Crofer22APU alloy and its analogs.

ACKNOWLEDGMENTS

The authors are grateful to A.S. Farlenkov for the assistance in performing microstructural studies.

This study was financially supported by the project the Russian Foundation for Basic Research and Belarussian Republican Foundation for Basic Research (grant nos. 17-58-04116 and Kh17RM-033, respectively) and of the Resolution of the Russian Federation Government no. 218 on Contract no. 02.G25.31.0198, Development and Setting up of High-Tech Production of Wide-Purpose Autonomous Current Sources Based on Domestic High-Performance Solid Oxide Fuel Cells. The research

was partially performed using the facilities of the Shared Access Centre "Composition of Compounds."

REFERENCES

1. Höland, W. and Beall, G., *Class-Ceramic Technology*, New Jersey: Wiley, 2012.
2. Smeacetto, F., Miranda, A., Chrysanthou, A., et al., *J. Am. Ceram. Soc*., 2014, vol. 97, no. 12, pp. 3835−3842.
3. Gurbinder, K., *Solid Oxide Fuel Cell Components,* Switzerland: Springer, 2016.
4. Mahato, N., Banerjee, A., Gupta, A., et al., *Prog. Mater. Sci*., 2015, vol. 72, pp. 141−337.
5. Lessing, P.A., *J. Mater. Sci*., 2007, vol. 42, no. 10, pp. 3465−3476.
6. Maharapta, M.K. and Lu, K., *Mater. Sci. Eng. R*, 2010, vol. 67, pp. 65−85.
7. Ley, K.L., Krumplet, M., Kumar, R., et al., *J. Mater. Res*., 1996, vol. 11, pp. 1489−1493.
8. Eichler, K., Solow, G., Otschik, P., et al., *J. Eur. Ceram. Soc*., 1999, vol. 19, pp. 1101−1104.
9. Sohn, S.B. and Choi, S.Y., *J. Am. Ceram. Soc*., 2004, vol. 87, pp. 254−260.
10. Larsen, P.H. and James, P.F., *J. Mater. Sci.,* 1998, vol. 33, pp. 2499−2507.
11. Nielsen, K.A., Solvang, M., Nielsen, S.B.L., et al., *J. Eur. Ceram. Soc*., 2007, vol. 27, pp. 1817−1822.
12. Chou, Y.S., Stewenson, J.W., and Choi, J.P., *Int. J. Appl. Ceram. Technol*., 2013, vol. 10, no. 1, pp. 97−106.
13. Donald, I.W., Mallison, P.M., Metcalfe, B.L., et al., *J. Mater. Sci*., 2011, vol. 46, pp. 1975−2000.
14. Reddy, A.A., Tulyaganov, D.U., Pascular, M.J., et al., *Int. J. Hydrogen Energy*, 2013, vol. 38, pp. 3073−3086.
15. Chou, Y.-S., Thomsen, E.C., Williams, R.T., et al., *J. Power Sources*, 2011, vol. 196, pp. 2709−2716.
16. Chou, Y.-S., Thomsen, E. C., Choi, J.-P., and Stevenson, J.W., *J. Power Sources*, 2012, vol. 197, pp. 154−160.
17. Chou, Y.-S., Stevenson, J.W., and Choi, J.-P., *J. Power Sources*, 2014, vol. 255, pp. 1−8.
18. Qi, S., Porotnikova, N.M., Ananyev, M.V., et al., *Trans. Nonferrous Met. Soc. China*, 2016, vol. 26, pp. 2916−2924.
19. Wang, J., Liu, C., Zhang, G., et al., *J. Non-Cryst. Solids*, 2015, vol. 419, pp. 1−5.